Explaining electron and muon $g − 2$ anomalies in an
Aligned 2-Higgs Doublet Model with Right-Handed Neutrinos

Luigi Delle Rose*

Institut de Fisica d'Altes Energies (IFAE), The Barcelona Institute of Science and Technology,
Campus UAB, 08193 Bellaterra (Barcelona), Spain and
School of Physics and Astronomy, University of Southampton, Southampton, SO17 1BJ, United Kingdom

Shaaban Khalil†

Center for Fundamental Physics, Zewail City of Science and Technology, 6 October City, Giza 12588, Egypt

Stefano Moretti‡

School of Physics and Astronomy, University of Southampton, Southampton, SO17 1BJ, United Kingdom

We explain anomalies currently present in various data samples used for the measurement of the anomalous magnetic moment of electron (a_e) and muon (a_μ) in terms of an Aligned 2-Higgs Doublet Model with right-handed neutrinos. The explanation is driven by one and two-loop topologies wherein a very light CP-odd neutral Higgs state (A) contributes significantly to a_μ but negligibly to a_e, so as to revert the sign of the new physics corrections in the former case with respect to the latter, wherein the dominant contribution is due to a charged Higgs boson ($H^\pm$) and heavy neutrinos with mass at the electroweak scale. For the region of parameter space of our new physics model which explains the aforementioned anomalies we also predict an almost background-free smoking-gun signature of it, consisting of $H^\pm A$ production followed by Higgs boson decays yielding multi-τ final states, which can be pursued at the Large Hadron Collider.

I. INTRODUCTION

It is tempting to conclude that the time-honoured discrepancy between the Standard Model (SM) prediction for the muon anomalous magnetic moment and its experimental measurement is a firm indication of New Physics (NP) Beyond the SM (BSM). Moreover, after improving the determination of the fine structure constant, it recently turned out that there is also a significant difference between the experimental result of the electron anomalous magnetic moment and the corresponding SM prediction. According to the latest results, we have the following deviations in the anomalous magnetic moments of muon and electrons [1, 2]:

$$\delta a_\mu = a_\mu^{\text{exp}} - a_\mu^{\text{SM}} = (278 \pm 88) \times 10^{-11} \,,$$
$$\delta a_e = a_e^{\text{exp}} - a_e^{\text{SM}} = (-87 \pm 36) \times 10^{-14}, \tag{1}$$

which indicate a 3.1σ and 2.4σ discrepancy between theory and experiment, respectively. Fermilab and J-PARC experiments [3, 4] are going to explore these anomalies in the near future with much higher precision, but now it is worthwhile speculating what possible NP phenomena might lie behind these two measurements. In doing so, it should be noted that δa_e and δa_μ have opposite signs, which provides a challenge for any BSM explanation attempting to account for both of them simultaneously. This generated growing interest and several extensions of the SM have been analysed as possible origin of the results in (1).

It is clear that any Electro-Weak (EW) scale NP effects that may explain the a_μ result will lead to corrections to a_e of order 10^{-5} times smaller, due to the typical relative suppression generated by the mass ratio $(m_e/m_\mu)^2$, and, crucially, with the same sign. Therefore, the anomalies of a_μ and a_e cannot be resolved simultaneously with the same NP contribution, unless it violates lepton flavour universality in a very peculiar way, so as to give a positive contribution to a_μ and a negative one to a_e. Some attempts along this line were in fact pursued by Ref. [5–26].

In this paper, we analyse the anomalous magnetic moment of muon and electron in a 2HDM with RH neutrinos and aligned Yukawa couplings. We emphasise that, in this class of models, one can account for the a_e through one-loop effects generated by the exchange of RH neutrinos and charged Higgs bosons. At the same time, the measured value of a_μ can be obtained accurately through two-loop effects generated by a light CP-odd neutral Higgs state in

combination with charged leptons. This phenomenology requires the $H^\pm$ and A states to be relatively light, so that their pair production process has a sizeable cross section at the Large Hadron Collider (LHC), thereby enabling one to fingerprint this A2HDM with RH neutrinos in the years to come.

The plan of this paper is as follows. In the next section we describe our NP scenario. In the following one we present the formulae for a_e and a_μ. After this, we present our results for the two anomalous magnetic moments and the aforementioned $H^\pm A$ signature in two separate subsections. We then conclude.

II. A2HDM WITH RH NEUTRINOS

The most general Yukawa Lagrangian of the 2HDM can be written as

$$-\mathcal{L}_Y = \bar{Q}'_L \left(Y'_{1d}\Phi_1 + Y'_{2d}\Phi_2\right) d'_R + \bar{Q}'_L \left(Y'_{1u}\tilde{\Phi}_1 + Y'_{2u}\tilde{\Phi}_2\right) u'_R + \bar{L}'_L \left(Y'_{1\ell}\Phi_1 + Y'_{2\ell}\Phi_2\right) \ell'_R$$
$$+ \bar{L}'_L \left(Y'_{1\nu}\tilde{\Phi}_1 + Y'_{2\nu}\tilde{\Phi}_2\right) \nu'_R + \text{h.c.}, \tag{2}$$

where the quark Q'_L, u'_R, d'_R and lepton L'_R, ℓ'_R, ν'_R fields are defined in the weak interaction basis and we also included the couplings of the Left-Handed (LH) lepton doublets with the RH neutrinos. The $\Phi_{1,2}$ fields are the two Higgs doublets in the Higgs basis and, as customary, $\tilde{\Phi}_i = i\sigma^2\Phi_i^*$. The Yukawa couplings Y'_{1j} and Y'_{2j}, with $j = u, d, \ell$, are 3×3 complex matrices while $Y'_{1\nu}$ and $Y'_{2\nu}$ are $3 \times n_R$ matrices, with n_R being the number of RH neutrinos. Besides implementing the standard Z_2 symmetry, potentially dangerous tree-level Flavour Changing Neutral Currents (FCNCs) can be tamed by requiring the alignment in flavour space of the two Yukawa matrices that couple to the same right-handed quark or lepton. This implies[1]

$$Y'_{2,d} = \zeta_d Y'_{1,d} \equiv \zeta_d Y'_d, \qquad Y'_{2,u} = \zeta_u Y'_{1,u} \equiv \zeta_u Y'_u, \qquad Y'_{2,\ell} = \zeta_\ell Y'_{1,\ell} \equiv \zeta_\ell Y'_\ell, \qquad Y'_{2,\nu} = \zeta_\nu Y'_{1,\nu} \equiv \zeta_\nu Y'_\nu. \tag{3}$$

Renormalisation group effects can introduce some misalignment in the Yukawa couplings. These provide negligible FCNC contributions in the quark sector suppressed by mass hierarchies $m_q m_{q'}^2/v^3$ [27, 28].

Aligned	Type I	Type II	Type III	Type IV
ζ_u	$\cot\beta$	$\cot\beta$	$\cot\beta$	$\cot\beta$
ζ_d	$\cot\beta$	$-\tan\beta$	$-\tan\beta$	$\cot\beta$
ζ_l	$\cot\beta$	$-\tan\beta$	$\cot\beta$	$-\tan\beta$

TABLE I. Relation between the ζ_f couplings of the A2HDM and the ones of the Z_2 symmetric scenarios.

The Yukawa Lagrangian in Eq. (2) generates a Dirac mass matrix for the standard neutrinos and can also be supplemented by a Majorana mass term M'_R for the RH ones

$$-\mathcal{L}_{M_R} = \frac{1}{2}\nu'^T_R C M'_R \nu'_R + \text{h.c.}, \tag{4}$$

where C is the charge-conjugation operator. In particular, by exploiting a bi-unitary transformation in the charged lepton sector and a unitary transformation on the RH neutrinos, $L'_L = U_L L_L$, $\ell'_R = U^\ell_R \ell_R$ and $\nu'_R = U^\nu_R \nu_R$, it is always possible to diagonalise (with real eigenvalues) the charged lepton and Majorana mass matrices at the same time,

$$U^\dagger_L Y'_\ell U^e_R = Y_\ell \equiv \frac{\sqrt{2}}{v}\text{diag}(m_e, m_\mu, m_\tau)\,,$$
$$U^{\nu\,T}_R M'_R U^\nu_R = M_R \equiv \text{diag}(M_1, \dots M_{n_R}), \tag{5}$$

while $Y_\nu = U^\dagger_L Y'_\nu U^\nu_R$ remains non-diagonal. In this basis the neutrino mass matrix can be written as

$$-\mathcal{L}_{\mathcal{M}_\nu} = \frac{1}{2}N^T_L C\mathcal{M}N_L + \text{h.c.} = \frac{1}{2}(\nu^T_L\, \nu^c_R{}^T)C \begin{pmatrix} 0 & M_D \\ M_D^T & M_R \end{pmatrix} \begin{pmatrix} \nu_L \\ \nu^c_R \end{pmatrix}, \tag{6}$$

---

[1] We have assumed real ζ_f. Notice also that the alignment in the neutrino sector is not a a consequence of the requirement of the absence of FCNCs. Nevertheless, we assume that the same mechanism that provides the alignment in the SM flavour space also holds for neutrinos.
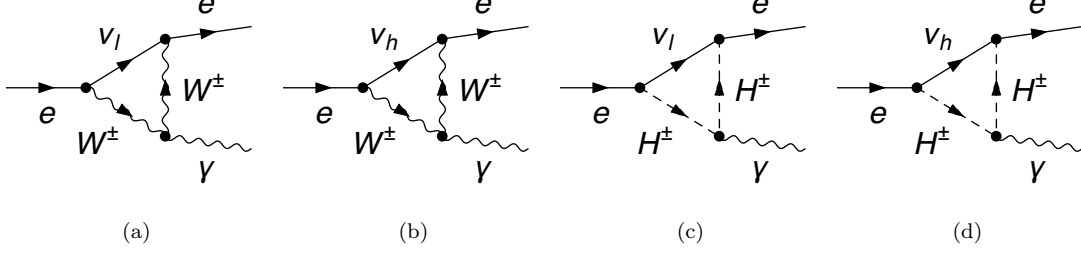
FIG. 1. Relevant Feynman diagrams contributing to the $g-2$ of the electron at one-loop order. Only the charges vector ($W^\pm$) and charged Higgs ($H^\pm$) currents are shown.

with $M_D = \frac{v}{\sqrt{2}} Y_\nu^*$ being the neutrino Dirac mass. This can be diagonalised with a unitary $(3+n_R) \times (3+n_R)$ matrix U, via

$$\begin{pmatrix} \nu_L \\ \nu_R^c \end{pmatrix} = U \begin{pmatrix} \nu_l \\ \nu_h \end{pmatrix} \equiv \begin{pmatrix} U_{Ll} & U_{Lh} \\ U_{R^c l} & U_{R^c h} \end{pmatrix} \begin{pmatrix} \nu_l \\ \nu_h \end{pmatrix}, \tag{7}$$

such that $\mathcal{M}_\nu = U^T \mathcal{M} U$ provides the masses of the three light active neutrinos ν_l and of the remaining n_R heavy sterile neutrinos ν_h.

The Yukawa interactions of the physical (pseudo)scalars[2] with the mass eigenstate fermions are then described by

$$-\mathcal{L}_Y = \frac{\sqrt{2}}{v} \bigg[\bar{u}(-\zeta_u\, m_u\, V_{ud}\, P_L + \zeta_d\, V_{ud}\, m_d\, P_R)d + \bar{\nu}_l(-\zeta_\nu\, m_{\nu_l}\, U_{Ll}^\dagger\, P_L + \zeta_\ell\, U_{Ll}^\dagger\, m_\ell\, P_R)\ell$$

$$+ \bar{\nu}_h(-\zeta_\nu\, m_{\nu_h}\, U_{Lh}^\dagger\, P_L + \zeta_\ell\, U_{Lh}^\dagger\, m_\ell\, P_R)\ell \bigg] H^+ + \text{h.c.}$$

$$+ \frac{1}{v} \sum_{\phi=h,H,A} \sum_{f=u,d,\ell} \xi_f^\phi\, \phi\, \bar{f}\, m_f\, P_R\, f + \frac{1}{v} \sum_{\phi=h,H,A} \xi_\nu^\phi\, \phi(\bar{\nu}_l\, U_{Ll}^\dagger + \bar{\nu}_h\, U_{Lh}^\dagger)P_R(U_{Ll}\, m_{\nu_l}\, \nu_l^c + U_{Lh}\, m_{\nu_h}\, \nu_h^c) + \text{h.c.}, \tag{8}$$

where the couplings of the neutral Higgs states to the fermions are given by

$$\xi_{u,\nu}^\phi = \mathcal{R}_{i1} + (\mathcal{R}_{i2} - i\mathcal{R}_{i3})\zeta_u^*, \qquad \xi_{d,\ell}^\phi = \mathcal{R}_{i1} + (\mathcal{R}_{i2} + i\mathcal{R}_{i3})\zeta_{d,\ell}, \tag{9}$$

where the matrix $\mathcal{R}$ diagonalises the scalar mass matrix. Because of the alignment of the Yukawa matrices all the couplings of the (pseudo)scalar fields to fermions are proportional to the corresponding mass matrices, hence the A2HDM acronym. Therefore, this 2HDM realisation is notably different from the standard four Types [29–31], wherein the Yukawa couplings are fixed to well defined functions of the ratio of the Vacuum Expectation Values (VEVs) of the two Higgs doublets, denoted by $\tan\beta$, see Tab. I.

Then, the charged Higgs boson currents in the lepton sector are given by:

$$-\mathcal{L}_Y^{\text{CC}} = \frac{\sqrt{2}}{v}\zeta_\ell \left[(\bar{\nu}_l\, U_{Ll}^\dagger + \bar{\nu}_h\, U_{Lh}^\dagger)m_\ell\, P_R\, \ell \right] H^+ - \frac{\sqrt{2}}{v}\zeta_\nu \left[(\bar{\nu}_l\, U_{Ll}^\dagger\, m_{\nu_l} + \bar{\nu}_h\, U_{Lh}^\dagger\, m_{\nu_h})\, P_L\, \ell \right] H^+ + \text{h.c.} \tag{10}$$

Finally, the neutral and charged gauge boson interactions of the neutrinos are

$$\mathcal{L}_Z = \frac{g}{2\cos\theta_W}(\bar{\nu}_l\, U_{Ll}^\dagger + \bar{\nu}_h\, U_{Lh}^\dagger)\gamma^\mu(U_{Ll}\, \nu_l + U_{Lh}\, \nu_h)Z_\mu,$$

$$\mathcal{L}_W = -\frac{g}{\sqrt{2}} \left[(\bar{\nu}_l\, U_{Ll}^\dagger + \bar{\nu}_h\, U_{Lh}^\dagger)\gamma^\mu P_L\, \ell \right] W_\mu^+ + \text{h.c.} \tag{11}$$

We refer to [32] for further details on the model.

———

[2] Note that, in a generic 2HDM with complex Higgs doublet fields, of the initial 8 degrees of freedom, upon EW Symmetry Breaking (EWSB), 5 survive as physical Higgs states: 2 CP-even, h and H (with, conventionally, $m_h < m_H$), 1 CP-odd, A, and 2 charged ones with undefined CP, $H^\pm$.

III.   ANOMALOUS MAGNETIC MOMENTS

The one-loop contributions to the anomalous magnetic moment of either lepton are

$$a_\ell = \frac{G_F\, m_\ell^2}{4\sqrt{2}\pi^2}\left[g_{(a)} + g_{(b)} + g_{(c)} + g_{(d)} + g_{2\text{HDM}}\right], \tag{12}$$

where the individual terms are

$$g_{(a)} = 2\sum_{i=1}^{3}|(U_{Ll})_{\ell\, i}|^2\left[\frac{5}{6} + \frac{1}{6}\frac{m_\ell^2}{M_W^2}\right] + \mathcal{O}(m_\ell^4),$$

$$g_{(b)} = 2\sum_{i=1}^{n_R}|(U_{Lh})_{\ell\, i}|^2\left[\frac{5}{6} + \mathcal{G}_{W^\pm}\left(\frac{m_{\nu_{h_i}}^2}{M_W^2}\right)\right] + \mathcal{O}(m_\ell^2),$$

$$g_{(c)} = 2\sum_{i=1}^{3}|(U_{Ll})_{\ell\, i}|^2\left[-\frac{\zeta_\ell^2}{12}\frac{m_\ell^2}{M_{H^\pm}^2}\right] + \mathcal{O}(m_\ell^4),$$

$$g_{(d)} = 2\sum_{i=1}^{n_R}|(U_{Lh})_{\ell\, i}|^2\,\mathcal{G}_{H^\pm}\left(\frac{m_{\nu_{h_i}}^2}{M_{H^\pm}^2}\right) + \mathcal{O}(m_\ell^2),$$

$$g_{2\text{HDM}} = \mathcal{O}(m_\ell^2), \tag{13}$$

with

$$\mathcal{G}_{W^\pm}(x) = \frac{-x + 6x^2 - 3x^3 - 2x^4 + 6x^3\log x}{4(x-1)^4},$$

$$\mathcal{G}_{H^\pm}(x) = \frac{\zeta_\nu^2}{3}\mathcal{G}_{W^\pm}(x) + \zeta_\nu\zeta_l\frac{x(-1 + x^2 - 2x\log x)}{2(x-1)^3}. \tag{14}$$

The index of the contributions corresponds to the different subfigures in Fig. 1 where, for simplicity, we show only the diagrams determined by the charged currents. The contribution $g_{(a)}$ alone would exactly correspond to the SM case if it were not for the rescaling induced by the neutrino mixing matrix. Nevertheless, the constant terms in $g_{(a)}$ and $g_{(b)}$ sums up to the SM result of 5/3 due to the unitarity of such a mixing matrix. Therefore, these can be neglected since they do not contribute to the NP part. The term $g_{2\text{HDM}}$ contains all the neutral Higgs boson contributions which are typical of the 2HDM alone. These are typically suppressed by a factor of m_ℓ^2/m_ϕ^2, with ϕ being one of the neutral (pseudo)scalar states of the 2HDM.

We can then write the contribution to $(g-2)_\ell$, $\ell = e, \mu$, due to charged currents as follows:

$$a_\ell^\pm = a_\ell^{W^\pm} + a_\ell^{H^\pm} = \frac{G_F\, m_\ell^2}{2\sqrt{2}\pi^2}\sum_{i=1}^{n_R}|(U_{Lh})_{\ell\, i}|^2\left[\mathcal{G}_{W^\pm}\left(\frac{m_{\nu_{h_i}}^2}{M_W^2}\right) + \mathcal{G}_{H^\pm}\left(\frac{m_{\nu_{h_i}}^2}{M_{H^\pm}^2}\right)\right]. \tag{15}$$

The contribution to $(g-2)_\ell$, $\ell = e, \mu$, from the neutral (pseudo)scalars is

$$a_\ell^0 = \sum_{\phi=h,H,A} a_\ell^\phi = \frac{G_F\, m_\ell^2}{4\sqrt{2}\pi^2}\sum_{\phi=h,H,A}(\xi_\ell^\phi)^2\frac{m_\ell^2}{m_\phi^2}\mathcal{F}_\phi\left(\frac{m_\ell^2}{m_\phi^2}\right), \tag{16}$$

where

$$\mathcal{F}_h(x) = F_H(x) \simeq -\frac{7}{6} - \log x, \qquad \mathcal{F}_A(x) \simeq \frac{11}{6} + \log x. \tag{17}$$

For the sake of completeness, we also give the Barr-Zee two-loop diagram contributions, [33–38]

$$a_\ell^{\text{two-loop}} = \frac{G_F m_\ell^2\alpha}{4\sqrt{2}\pi^3}\sum_{\phi=h,H,A}\sum_{f}N_c^f Q_f^2\xi_\ell^\phi\xi_f^\phi\frac{m_\ell^2}{m_\phi^2}G_\phi\left(\frac{m_\ell^2}{m_\phi^2}\right), \tag{18}$$

where N_c^f is the number of colours and Q_f the electric charge while

$$G_\phi(x) = \int_0^1 dz\frac{\tilde{g}_\phi(z)}{z(1-z)-x}\log\frac{z(1-z)}{x}, \qquad \text{with}\quad \tilde{g}_\phi(z) = \begin{cases} 2z(1-z)-1, & \phi=h,H \\ 1, & \phi=A \end{cases}. \tag{19}$$

The total contribution to the $g-2$ is thus given by $a_\ell = a_\ell^\pm + a_\ell^0 + a_\ell^{\text{two-loop}}$.

Finally we present the Branching Ratio (BR) of the Lepton Flavour Violating (LFV) decays $\ell_\alpha \to \ell_\beta \gamma$ (with $\alpha, \beta = e, \mu, \tau$), as follows:

$$\text{BR}(\ell_\alpha \to \ell_\beta \gamma) = \mathcal{C} \left| \sum_{i=1}^{n_R} (U_{Lh}^*)_{\alpha i}(U_{Lh})_{\beta i} \left[\mathcal{G}_{W^\pm}\left(\frac{m_{\nu_{h_i}}^2}{M_W^2}\right) + \mathcal{G}_{H^\pm}\left(\frac{m_{\nu_{h_i}}^2}{M_{H^\pm}^2}\right) \right] \right|^2, \tag{20}$$

with

$$\mathcal{C} = \frac{\alpha_W^3 s_W^2}{256\pi^2}\left(\frac{m_{\ell_\alpha}}{M_W}\right)^4 \frac{m_{\ell_\alpha}}{\Gamma_{\ell_\alpha}}, \tag{21}$$

where Γ_{ℓ_α} is the total decay width of the lepton ℓ_α and the loop functions are given above. The structure of the loop corrections is obviously the same as the one appearing above in the charged current corrections to $(g-2)_\ell$. The measured BR of these LFV decays will act as a constraint in our analysis.

IV.   RESULTS

The solution of the a_μ anomaly relies upon a light pseudoscalar state A contributing to the dominant two-loop Barr-Zee diagrams, as customary in 2HDMs. The explanation of the anomaly is particularly simple in the 'lepton-specific' 2HDM scenario, also dubbed Type-IV, in which the couplings of the A and $H^\pm$ bosons to the leptons can be enhanced (for large $\tan\beta$) while those to the quarks are suppressed (being proportional to $\tan^{-1}\beta$). Indeed, while it is always possibile to enhance the couplings to the leptons in any of the four standard realisations of the 2HDM, in Type-I and -III this is done at the cost of increasing the couplings to the up quark (for small $\tan\beta$). As a consequence, one faces a strong constraint from the perturbativity of the top-quark Yukawa coupling. In the Type-II, instead, the couplings to the down-quarks are enhanced (for large $\tan\beta$) and severe bounds are imposed by flavour physics and direct searches for extra Higgs bosons. These issues can be much more easily addressed in the A2HDM since the couplings to leptons and quarks are disentangled and ζ_ℓ can be raised independently of ζ_u and ζ_d.

It is worth emphasising that a simultaneous explanation of both the a_e and a_μ anomalies cannot be achieved neither in the Z_2 symmetric scenarios of the 2HDM nor in the pure A2HDM, since the contributions to the anomalous moments have a fixed sign as they both originate from the same ζ_ℓ. In [26], this constraint has been overcome by decoupling the electron and muon sectors, where all Yukawa matrices can be made diagonal in the fermion mass basis [39, 40]. Here, instead, the degeneracy will be broken by exploiting the lepton non-universality that naturally arises in RH neutrino models: augmenting the A2HDM with RH neutrinos can allow for an independent solution to a_e. This is obtained with the one-loop diagrams shown in Fig. 1 provided that the charged Higgs boson is not too heavy to suppress the loop corrections.

The mass of the charged Higgs boson is bounded from below by direct searches at LEP II. In particular, searches for $H^\pm$ pair production provide $m_{H^\pm} \gtrsim 93.5$ GeV at 95 % Confidence Level (CL) [41] assuming the charged Higgs only decays leptonically into $\tau\nu$. Since the mass of the pseudoscalar A state is thus required to be much lighter than the charged one, our scenarios realises the mass hierarchy $m_A \ll m_{H^\pm} \simeq m_H$. The almost degeneracy between the heavy neutral scalar and the charged Higgs state is induced by the constraints on the EW Precision Observables (EWPOs), i.e., S, T and U. Indeed, the most stringent one arises from custodial symmetry and reads as[3]

$$\Delta T \simeq \frac{m_H}{32\pi^2\alpha v^2}(m_{H^\pm} - m_H), \tag{22}$$

which fixes the mass splitting to $(m_{H^\pm} - m_H) \sim \mathcal{O}(10$ GeV$)$.

As quoted above, the scenarios with light scalar states is strongly constrained by flavour physics, in particular by neutral meson mixings (ΔM_q and ϵ_K), leptonic decays of neutral and charged mesons as well as radiative B decays ($b \to s\gamma$). These mostly depend on $m_{H^\pm}$, $\zeta_{u,d}$. Such measurements are reconciled in our setup simply by requiring a sufficiently small $\zeta_{u,d}$ which we will set to zero for the sake of simplicity. This in turn implies that the Yukawa interactions in our BSM scenario are purely leptophilic. This configuration also naturally complies with void searches for extra (pseudo)scalars at the LHC. In this respect, we have required that the Higgs sector of our model is compliant with the experimental constraints implemented in HiggsSignals [42] (capturing the LHC measurements

---

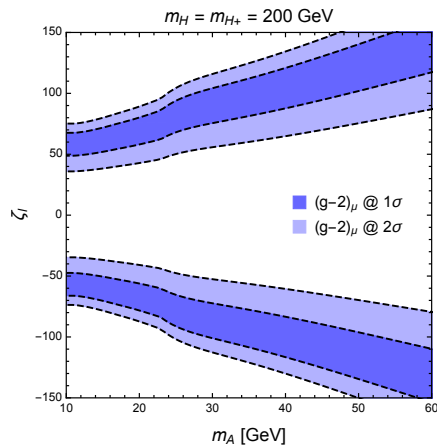[3] The expression for ΔT assumes the mass hierarchy $m_A \ll m_Z \ll m_{H^\pm} \simeq m_H$ and $\sin(\beta - \alpha) \simeq 1$.

FIG. 2. The 1 and 2σ regions of the anomalous magnetic moment of the muon in the parameter space of m_A and ζ_ℓ. For the sake of definiteness, the mass of the charged Higgs has been chosen as $m_{H^\pm} = 200$ GeV.

of the discovered Higgs boson[4]) and in HiggsBounds [43] (enforcing limits following the aforementioned void searches for the H, A and $H^\pm$ states at past and present colliders).

Contributions mediated by the charged Higgs states also affect the leptonic decays $\ell_i \to \ell_j \nu \bar{\nu}$ at tree level, with the stronger constraint coming from $\tau \to \mu \nu \bar{\nu}$ [44, 45]. The corresponding bound projects onto the ratio $z = \zeta_\ell^2 \, m_\tau m_\mu / m_{H^\pm}^2$ and gives $|z| < 0.72$ at 95% CL [46].

Finally, upper bounds on LFV processes, (BR($\mu \to e\gamma$) $\leq 4.2 \times 10^{-13}$, BR($\tau \to e\gamma$) $\leq 3.3 \times 10^{-8}$, BR($\tau \to \mu\gamma$) $\leq 4.4 \times 10^{-8}$ at 90% CL) constrain the RH neutrinos interactions with the charged leptons. The charged Higgs boson also affects these decays with a large contribution. Since a RH neutrino is only employed in the explanation of the a_e anomaly, a non-negligible mixing is strictly required with the electron family. Therefore, the stringent constraint from $\mu \to e\gamma$ and the milder one from $\tau \to e\gamma$ can be satisfied by simply relying on the hierarchy $|(U_{Lh})_{\tau \, \nu_h}|, |(U_{Lh})_{\mu \, \nu_h}| \ll |(U_{Lh})_{e \, \nu_h}|$.

A. Predictions for δa_e and δa_μ

The contribution to δa_e arising from the $W^\pm$, encoded in the $\mathcal{G}_{W^\pm}$ function defined in Eq. (14), is negative but it can never be enhanced being fixed by the gauge interactions. For $m_{\nu_{h_i}}^2 / M_W^2 \gg 1$, $\mathcal{G}_{W^\pm} \simeq -1/2$. The impact of the charged Higgs boson in the loop functions is, however, much different. As an example, for large heavy neutrino masses, it saturates to $\mathcal{G}_{H^\pm} \simeq \zeta_\ell \zeta_\nu / 2 - \zeta_\nu^2 / 6$ or behaves as $\mathcal{G}_{H^\pm} \simeq (\zeta_\ell \zeta_\nu / 2 - \zeta_\nu^2 / 12)(m_{\nu_h}^2 / m_{H^\pm}^2)$ for larger $m_{H^\pm}$. In both cases, the solution of the a_e anomaly is facilitated by large and opposite ζ_ℓ and ζ_ν. The same effect would also push the predicted a_μ in the opposite direction with respect to the current measurement. This is not an issue since the same hierarchy $|(U_{Lh})_{\mu \, \nu_h}| \ll |(U_{Lh})_{e \, \nu_h}|$ required to prevent the LFV bounds also suppresses the contribution of the charged Higgs boson to the muon $g-2$. As well known in the literature, the latter can be explained in the 2HDM by the two-loop Barr-Zee diagrams of the neutral scalars which provide a positive correction for sufficiently light A. This contribution may compete in a_e against the one-loop effects discussed above but it is found to be subdominant in most of the parameter space.

The results of our analysis are depicted in Figs. 2 and 3. The former shows the regions in which the predicted a_μ is within 1 and 2σ around the measured central value. These are projected onto the most relevant parameter space defined by m_A and ζ_ℓ. The mass of the charged Higgs boson has been fixed at a reference value of $m_{H^\pm} = 200$ GeV. Different choices of $m_{H^\pm}$ slightly modify the contours shown in the plot. In Fig. 3 we show the prediction for a_e. The points are generated by scanning over the parameter space of the model and comply with the experimental and theoretical bounds quoted above while reproducing a_μ within the 2σ range. The parameters are scanned as follows: $m_{\nu_h} \in (200, 2000)$ GeV, $m_{H^\pm}, m_H \in (100, 1000)$ GeV, $m_A \in (10, 60)$ GeV, $\zeta_\ell, \zeta_\nu \in (-150, 150)$ and $|(U_{Lh})_{\mu \, \nu_h}|^2 \in (10^{-5}, 10^{-3})$. In Fig. 3(a) and (b), $(g-2)_e$ is plotted, respectively, against ζ_ν and the effective coupling $\zeta_\nu Y_\nu$ which characterises this model and that has been extensively discussed in [32]. The vertical dashed line shows the maximum
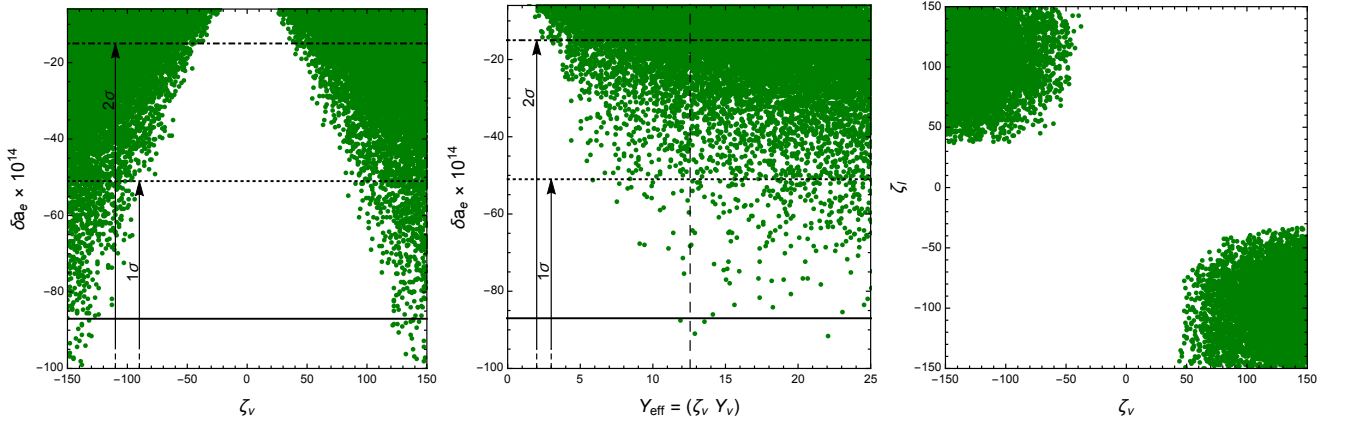
---

[4] In our BSM scenario this is the h state.

FIG. 3. The anomalous magnetic moment of the electron as a function of (a) ζ_ν and (b) the effective neutrino coupling $\zeta_\nu Y_\nu$. The horizontal solid, dashed and dot-dashed lines correspond, respectively, to the central value, the upper 1σ band and the upper 2σ band. The vertical dashed line in (b) represents the maximum allowed value for $Y_{\rm eff} = \zeta_\nu Y_\nu$ from perturbativity. All the points satisfy the experimental and theoretical constraints as explained in the text and reproduce a_μ at 2σ level. (c) Distribution of points in the (ζ_ν, ζ_ℓ) plane complying with all current experimental and theoretical bounds as well as with the solution of the a_e and a_μ anomalies at 2σ.

allowed value required by pertubativity. Finally, Fig. 3(c) shows the distribution of points along the ζ_ν and ζ_ℓ directions compliant with all the bounds discussed above as well as a_e and a_μ measurements within 2σ. As mentioned already, the two couplings must necessarily have opposite signs.

B. LHC phenomenology of the extra (pseudo)scalar bosons

In the leptophilic scenario delineated above, the light pseudoscalar state A can decay at tree-level via $A \to \tau\tau$ with BR close to 100%. For the charged Higgs boson, instead, the two main open decay modes are $H^\pm \to AW^\pm$, where the interaction is completely fixed by the $SU(2)_L$ gauge coupling, and $H^\pm \to \tau^\pm\nu$, which is controlled by the ζ_ℓ coupling. Analogously, for the heavy neutral scalar state H the two leading decay modes are $H \to \tau\tau$ and $H \to AZ$. For large $m_{H^\pm}, m_H$, the BRs of the $H^\pm$ and H are solely controlled by the coupling $g_\ell = \zeta_\ell\, m_\tau/m_{H^\pm}$ and are approximated by[5]

$$\mathrm{BR}(H^\pm \to AW^\pm) = \mathrm{BR}(H \to AZ) = \frac{1}{1 + 2g_\ell^2}, \qquad \mathrm{BR}(H^\pm \to \tau^\pm\nu) = \mathrm{BR}(H \to \tau\tau) = \frac{2g_\ell^2}{1 + 2g_\ell^2}. \tag{23}$$

Since the couplings to the quarks are suppressed, the main production modes proceed through the EW interactions. The relevant processes are

$$pp \to H^\pm A, \qquad pp \to HA, \qquad pp \to H^\pm H, \qquad pp \to H^+ H^-, \tag{24}$$

with the corresponding cross sections being only functions of the masses of the corresponding particles. The cross sections at the LHC are computed with MadGraph [47] and are shown in Fig. 4. The largest contributions arise from $H^\pm A$ and HA.

The main signatures resulting from these processes are characterised by final states with several τ leptons

$$3\tau + \not{E}_T, \qquad 4\tau + W^\pm, \qquad 4\tau, \qquad 4\tau + Z, \tag{25}$$

where the first two stem from $H^\pm A$ production (with a subleading component from $H^\pm H$) while the last two arise from the HA production. A thorough analysis is beyond the scope of this paper. In order to get a feeling of the potential of these channels, here we list only an estimate of the inclusive cross section for the corresponding SM background

$$\sigma_{\rm SM}(ZW^\pm \to 3\tau + \not{E}_T) \simeq 94\,{\rm fb}, \qquad \sigma_{\rm SM}(ZZW^\pm \to 4\tau + W^\pm) \simeq 3.2 \times 10^{-2}\,{\rm fb},$$
$$\sigma_{\rm SM}(ZZ \to 4\tau) \simeq 11\,{\rm fb}, \qquad \sigma_{\rm SM}(ZZZ \to 4\tau + Z) \simeq 1.1 \times 10^{-2}\,{\rm fb}. \tag{26}$$

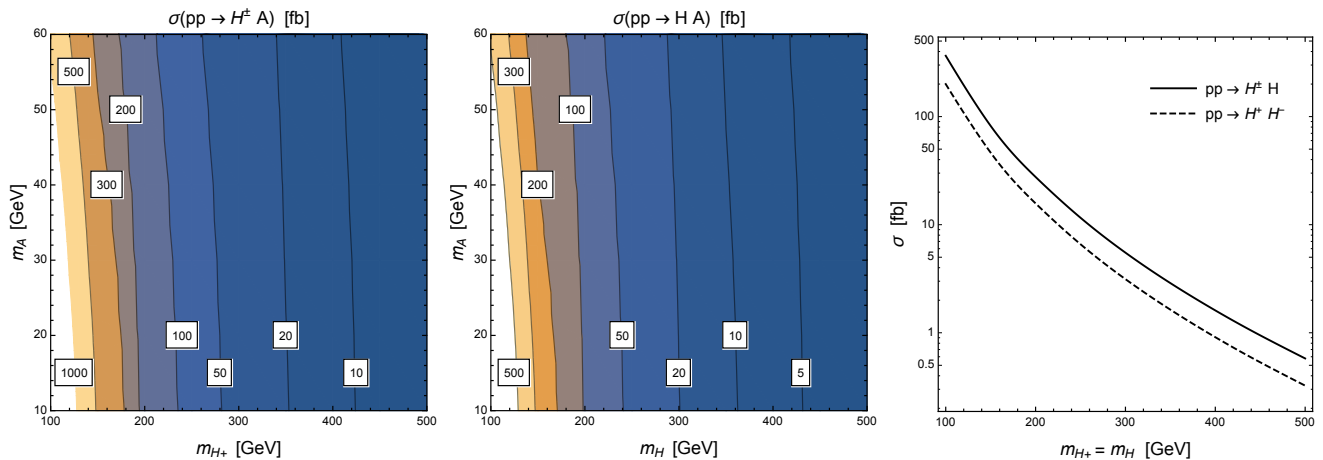[5] We neglected small deviations from $\sin(\beta - \alpha) = 1$.

FIG. 4. The LHC production cross sections of pairs of the extra Higgs bosons as functions of m_A and $m_{H^\pm} = m_H$.

V. CONCLUSIONS

The measurements of the the anomalous magnetic moment of electron and muon are amongst the most precise ones in the whole of particle physics, probing not only the structure of the SM but also the possibility of BSM theories entering these experimental observables. Intriguingly, both of these are currently showing some anomalies with respect to the SM predictions. Crucially, the two results go in different directions, i.e., the measurement of a_μ exceeds the SM result while that of a_e lies below the corresponding SM yield. This circumstance makes it difficult to find BSM solutions, as multiple new particles are generally needed, each contributing its corrections in different directions, i.e., with different signs, unless significant violation of discrete quantum numbers is exploited.

In this paper, we adopted an A2HDM supplemented by RH neutrinos, respecting all the SM symmetries. In such a BSM framework, a possible explanation to the aforementioned anomalies can be attained through one and two-loop topologies wherein the contribution from a very light CP-odd neutral Higgs state interacting with leptons, is tensioned against the one due to a charged Higgs boson interacting with the new heavy neutrinos, the latter with mass at the EW scale. Crucially, such a spectrum is able to explain the two leptonic anomalous magnetic moment measurements while also predicting new hallmark signals in the form of $q\bar{q}' \to H^\pm A$ production yielding multi-τ final states, which are almost background free at the LHC and thus accessible already with current data samples.

ACKNOWLEDGEMENTS

[1] A. Keshavarzi, W. J. Marciano, M. Passera, and A. Sirlin, Phys. Rev. D **102**, 033002 (2020), arXiv:2006.12666 [hep-ph].

[2] R. H. Parker, C. Yu, W. Zhong, B. Estey, and H. Müller, Science **360**, 191 (2018), arXiv:1812.04130 [physics.atom-ph].

[3] Y. Semertzidis *et al.*, in *KEK International Workshop on High Intensity Muon Sources (HIMUS 99)* (1999) pp. 81–96, arXiv:hep-ph/0012087.

[4] F. Farley, K. Jungmann, J. Miller, W. Morse, Y. Orlov, B. Roberts, Y. Semertzidis, A. Silenko, and E. Stephenson, Phys. Rev. Lett. **93**, 052001 (2004), arXiv:hep-ex/0307006.

[5] J. Liu, C. E. Wagner, and X.-P. Wang, JHEP **03**, 008 (2019), arXiv:1810.11028 [hep-ph].

[6] X.-F. Han, T. Li, L. Wang, and Y. Zhang, Phys. Rev. D **99**, 095034 (2019), arXiv:1812.02449 [hep-ph].

[7] M. Endo and W. Yin, JHEP **08**, 122 (2019), arXiv:1906.08768 [hep-ph].

[8] M. Bauer, M. Neubert, S. Renner, M. Schnubel, and A. Thamm, Phys. Rev. Lett. **124**, 211803 (2020), arXiv:1908.00008 [hep-ph].

[9] M. Badziak and K. Sakurai, JHEP **10**, 024 (2019), arXiv:1908.03607 [hep-ph].

[10] A. Cárcamo Hernández, Y. Hidalgo Velásquez, S. Kovalenko, H. Long, N. A. Pérez-Julve, and V. Vien, (2020), arXiv:2002.07347 [hep-ph].

[11] N. Haba, Y. Shimizu, and T. Yamada, PTEP **2020**, 093B05 (2020), arXiv:2002.10230 [hep-ph].

[12] I. Bigaran and R. R. Volkas, Phys. Rev. D **102**, 075037 (2020), arXiv:2002.12544 [hep-ph].

[13] L. Calibbi, M. López-Ibáñez, A. Melis, and O. Vives, JHEP **06**, 087 (2020), arXiv:2003.06633 [hep-ph].

[14] C.-H. Chen and T. Nomura, (2020), arXiv:2003.07638 [hep-ph].

[15] S. Jana, V. P. K., and S. Saad, Phys. Rev. D **101**, 115037 (2020), arXiv:2003.03386 [hep-ph].

[16] S.-P. Li, X.-Q. Li, Y.-Y. Li, Y.-D. Yang, and X. Zhang, (2020), arXiv:2010.02799 [hep-ph].

[17] E. J. Chun and T. Mondal, JHEP **11**, 077 (2020), arXiv:2009.08314 [hep-ph].

[18] S. Jana, P. Vishnu, W. Rodejohann, and S. Saad, Phys. Rev. D **102**, 075003 (2020), arXiv:2008.02377 [hep-ph].

[19] C. Arbeláez, R. Cepedello, R. M. Fonseca, and M. Hirsch, Phys. Rev. D **102**, 075005 (2020), arXiv:2007.11007 [hep-ph].

[20] L. Delle Rose, C. Marzo, and L. Marzola, (2020), arXiv:2005.12389 [hep-ph].

[21] A. Crivellin, M. Hoferichter, and P. Schmidt-Wellenburg, Phys. Rev. D **98**, 113002 (2018), arXiv:1807.11484 [hep-ph].

[22] B. Dutta, S. Ghosh, and T. Li, Phys. Rev. D **102**, 055017 (2020), arXiv:2006.01319 [hep-ph].

[23] C. Hati, J. Kriewald, J. Orloff, and A. Teixeira, JHEP **07**, 235 (2020), arXiv:2005.00028 [hep-ph].

[24] A. Cárcamo Hernández, S. King, H. Lee, and S. Rowley, Phys. Rev. D **101**, 115016 (2020), arXiv:1910.10734 [hep-ph].

[25] A. Crivellin and M. Hoferichter, in *An Alpine LHC Physics Summit 2019* (2019) pp. 29–34, arXiv:1905.03789 [hep-ph].

[26] F. J. Botella, F. Cornet-Gomez, and M. Nebot, Phys. Rev. D **102**, 035023 (2020), arXiv:2006.01934 [hep-ph].

[27] M. Jung, A. Pich, and P. Tuzon, JHEP **11**, 003 (2010), arXiv:1006.0470 [hep-ph].

[28] X.-Q. Li, J. Lu, and A. Pich, JHEP **06**, 022 (2014), arXiv:1404.5865 [hep-ph].

[29] J. F. Gunion, H. E. Haber, G. L. Kane, and S. Dawson, *The Higgs Hunter's Guide*, Vol. 80 (2000).

[30] J. F. Gunion, H. E. Haber, G. L. Kane, and S. Dawson, (1992), arXiv:hep-ph/9302272.

[31] G. Branco, P. Ferreira, L. Lavoura, M. Rebelo, M. Sher, and J. P. Silva, Phys. Rept. **516**, 1 (2012), arXiv:1106.0034 [hep-ph].

[32] L. Delle Rose, S. Khalil, S. J. King, and S. Moretti, Phys. Rev. D **101**, 115009 (2020), arXiv:1903.11146 [hep-ph].

[33] S. M. Barr and A. Zee, Phys. Rev. Lett. **65**, 21 (1990), [Erratum: Phys.Rev.Lett. 65, 2920 (1990)].

[34] A. Czarnecki, B. Krause, and W. J. Marciano, Phys. Rev. D **52**, 2619 (1995), arXiv:hep-ph/9506256.

[35] D. Chang, W.-Y. Keung, and T. Yuan, Phys. Rev. D **43**, 14 (1991).

[36] K.-m. Cheung, C.-H. Chou, and O. C. Kong, Phys. Rev. D **64**, 111301 (2001), arXiv:hep-ph/0103183.

[37] K. Cheung, O. C. Kong, and J. S. Lee, JHEP **06**, 020 (2009), arXiv:0904.4352 [hep-ph].

[38] A. Cherchiglia, P. Kneschke, D. Stöckinger, and H. Stöckinger-Kim, JHEP **01**, 007 (2017), arXiv:1607.06292 [hep-ph].

[39] A. Peñuelas and A. Pich, JHEP **12**, 084 (2017), arXiv:1710.02040 [hep-ph].

[40] F. J. Botella, F. Cornet-Gomez, and M. Nebot, Phys. Rev. D **98**, 035046 (2018), arXiv:1803.08521 [hep-ph].

[41] G. Abbiendi *et al.* (ALEPH, DELPHI, L3, OPAL, LEP), Eur. Phys. J. C **73**, 2463 (2013), arXiv:1301.6065 [hep-ex].

[42] P. Bechtle, S. Heinemeyer, O. Stål, T. Stefaniak, and G. Weiglein, Eur. Phys. J. C **74**, 2711 (2014), arXiv:1305.1933 [hep-ph].

[43] P. Bechtle, D. Dercks, S. Heinemeyer, T. Klingl, T. Stefaniak, G. Weiglein, and J. Wittbrodt, (2020), arXiv:2006.06007 [hep-ph].

[44] Y. Kuno and Y. Okada, Rev. Mod. Phys. **73**, 151 (2001), arXiv:hep-ph/9909265.

[45] T. Abe, R. Sato, and K. Yagyu, JHEP **07**, 064 (2015), arXiv:1504.07059 [hep-ph].

[46] P. Zyla *et al.* (Particle Data Group), PTEP **2020**, 083C01 (2020).

[47] J. Alwall, R. Frederix, S. Frixione, V. Hirschi, F. Maltoni, O. Mattelaer, H. S. Shao, T. Stelzer, P. Torrielli, and M. Zaro, JHEP **07**, 079 (2014), arXiv:1405.0301 [hep-ph].